Study on the temperature and strain fields in gas foil bearings – measurement method and numerical simulations

Indexed by:
Web of Science Group

Paweł Zdziebko [a],*, Adam Martowicz [a]

[a] AGH University of Science and Technology, Department of Robotics and Mechatronics, al. A. Mickiewicza 30, 30-059 Kraków, Poland

Highlights

- A method for measurement of the temperature and strain fields in the bearing's top foil making use of its specialized version equipped with sensors of the adequate physical quantities has been proposed.

- A numerical model of a gas foil bearing has been developed using the Finite Element Method, which takes into account thermomechanical couplings.

- The obtained results of numerical calculations have indicated the dominant directions of strains as well as temperature distribution in the bearing.

Abstract

Gas foil bearings belong to the group of slide bearings and are used in devices in which operation at high rotational speeds of the shafts are of key importance, e.g., in gas turbines. The air film developed on the surface of the bearing's top foil allows this structural component to be separated from the shaft. This ensures a non-contact operation of the bearing. In the case of the mentioned type of bearings, their resultant operational properties are influenced by both thermal and mechanical phenomena. The current work presents a model of a gas foil bearing developed making use of the Finite Element Method. The model takes into account thermomechanical couplings which are necessary for the correct simulation of the operation of physical components of the modeled system. The paper reports the results of numerical analyzes conducted for the elaborated model as well as the relevant conclusions concerning thermomechanical couplings present in gas foil bearings. The method for the experimental identification of the temperature and strain fields in the bearing's top foil proposed to validate the numerical model is also presented.

Keywords

gas foil bearing, numerical analysis, thermomechanical couplings, Finite Element Method, temperature field, strain field.

1. Introduction

Most of the machines used in the industry require bearings to support shafts. It is necessary to support them to provide the capability of both carrying loads and allowing rotation. The lifespan of the rotating machineries strongly depends on the technical condition and operating parameters of the used shafts' bearings. Hence, it should be noticed that a number of works related to the analysis of maintenance problems and ensuring the operational reliability of bearings have been published so far, e.g., [1, 14, 21]. In the work [8], the authors present a review of algorithms that enable the assessment of the bearing's degradation based on machine learning. The authors also conclude that there is still a lack of universal indicator that would allow for an unambiguous determination of the trend regarding bearing's degradation. On the other hand, the work [23] deals with the issue of type selection of the bearing ensuring correct operation of high-speed systems.

In the present work, the authors focus their research efforts on a specific type of the bearings, namely the gas foil bearings (GFB)s, also known as air foil bearings. These bearings are a subgroup of the slide bearings. However, in contrary to the typical slide bearings, in which the lubricating medium is usually oil, GFBs make use of air

[15]. A general view of the bearing's installation employing a GFB is schematically shown in Fig. 1A. The bearing's bushing is fixed in the housing by means of the thrust rings. The characteristic components of a GFB are the top foil and bump foils [19]. A close-up view showing the bearing's bushing, top and bump foils as well as the rotating shaft is shown in Fig. 1B.

In a GFB, the rotating shaft is supported by a top foil which, in turn, is held in a desired location in the bushing by the bump foils. The required gap between the shaft and the top foil is provided by the hydrodynamic pressure generated while developing the air film. Generation of this pressure is ensured by the fact that the air is drawn in (due to viscous effects) between the shaft and the top foil. A high rotational speed of the shaft with respect to the bearing's bushing is required to form a continuous air film. Once achieved, the generated air film enables non-contact operation of the bearing, which refers to the nominal condition of its maintenance.

As mentioned, the developing air film creates a small clearance, several micrometers thick, between the surface of the shaft's journal and the top foil. Through this gap, the air is continuously exchanged with the surroundings. Maintaining this gap is essential for the correct operation of the bearing [22]. However, the use of air as a lubricant in GFBs introduces certain limitations in terms of their use. The consid-

(*) Corresponding author.
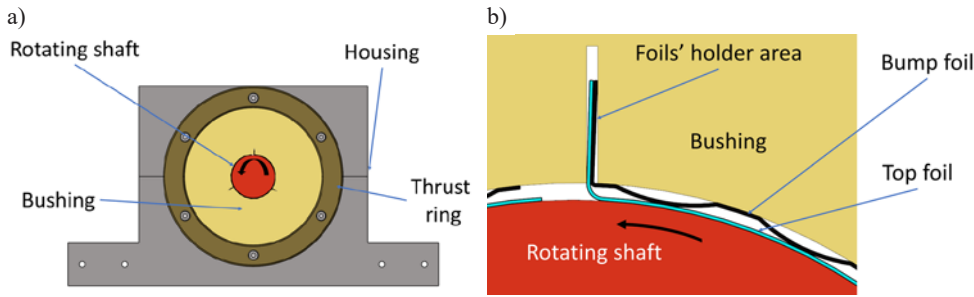E-mail addresses: P. Zdziebko - zdziebko@agh.edu.pl, A. Martowicz - adam.martowicz@agh.edu.pl

a)

b)

Fig. 1. Scheme of a GFB: a general view (a) and view of the top and bump foils arrangement (b)

Bagiński et al. [3] conducted research on the influence of GFB cooling on the dynamics of the entire rotor bearing system. A recirculating fan has proven to be the most effective way to cool a bearing. The experimentally identified temperature drops were the greatest compared to other examined cooling methods.

In this paper, the authors present a prototype of a top foil equipped with thermocouples and strain gauges, which in the course of further planned experi-

ered lubricating medium, i.e., the air, is characterized by a lower effective stiffness compared to the oils used in typical slide bearings. This property limits the bearing's ability to carry high loads. At the same time, however, it allows the use of GFBs in applications characterized by high rotational speeds of the supported shafts. Consequently, GFBs are especially dedicated to the high-speed and preferably lightly-loaded devices, e.g., air turbines.

The bump foils are the components in the structural part of the supporting layer in a GFB that ensure the required bearing's compliance [5, 20]. This characteristics of the bump foils enables the correct behavior of the bearing undergoing varying operational conditions, including the change of the load within its allowed range. Moreover, a slight misalignment between the shaft's and bearing's axes is also acceptable due to the above-mentioned mechanical property. The geometry of the supporting foils, i.e., their shape and thickness as well as their number are the subject of the ongoing research [9, 10]. Similarly, the manufacturing technologies dedicated for the GFB's foils are under constant development [6, 20].

The maintenance conditions set for GFBs during their steady state operation usually do not significantly affect the bearings' wear. Contrarily, the GFBs' transient states, i.e., the performed run-up and run-out cycles, are the key issue from the point of view of ensuring the operational reliability of the bearings. In fact, during these states the bearing's shaft temporarily remains in a direct mechanical contact with the top foil, hence, experiencing a dry friction. In order to improve the GFB's operational conditions during the transient states, additional protective layers with a low friction coefficient, e.g., made of ceramics, are sputtered on the inner surfaces of top foils. Nevertheless, when the bearing operates under incorrect supporting conditions or with the wrong direction of rotation of the shaft, the foil may jam on the shaft, and the abrasion of the top foil's protective layer may occur, as shown in Fig. 2.

There are currently conducted studies on developing technical solutions to improve the operational properties of GFBs and ensure their better reliability. Martowicz et al. [12] presented an extensive review of the applications of intelligent materials in order to improve the properties of GFBs or their adaptation to specific applications. In the work [17], the authors proposed a method of reducing the uneven temperature distribution in the top foil with the use of current-controlled thermoelectric modules. In the conducted analyzes, the modules were distributed axially and circumferentially in the bearing's bushing and controlled independently. The obtained results of the referenced research showed a positive effect of the proposed approach in reducing the unevenness of the temperature gradient in the top foil.

Fig. 2. Abrasion of the sputtered protective layer on the inner surface of the GFB's top foil

mental tests will allow identification of the temperature and strain fields in the mentioned type of the foil mounted in a GFB. According to the authors' knowledge, such research has not yet been conducted in a comprehensive manner. Moreover, the developed measurement system will enable monitoring of the bearing's operating conditions, which is very desirable. In order to better understand the nature of thermomechanical couplings in the examined GFB, the simulation model presented in this work has been developed. The use of the elaborated model by means of virtual analyzes will allow to determine and, therefore, predict the values expected to be recorded by the sensors during future laboratory tests. The prototype of the foil-sensor described in Chapter 2 is the result of the several-year-long research conducted by the authors. Based on the previous experiences reported in [11, 13], an innovative concept of the temperature measurement technique making use of the in-house manufactured thermocouples was recently presented in [18]. Moreover, the proposed prototype of the foil-sensor is equipped with strain gauges that allow to measure the strain field. Their indications will be examined in the future in terms of the presence of unfavorable operating conditions of the GFB, for example not to let the top foil jam on the shaft. The measurements will also make it possible to determine the

directions of the dominant strains of the top foil during the bearing's operation. Its deformations can significantly affect the reliability of the GFB's operation, which is the overall subject of the conducted research. It should be noted that the computational model discussed in Chapter 3 takes into account thermomechanical couplings, which enable characterization of the course of the deformation process of the foils in a GFB using numerical simulations. Chapter 4 presents the results of the conducted analyzes, while Chapter 5 summarizes the study and sets out the planned directions for further work.

2. Foil-sensor prototype

The phenomena related to the deformations and temperature field in the top foil of a GFB have not been thoroughly investigated so far. The present works carried out by the authors meet the above-mentioned challenge. They proposed to develop and manufacture a dedicated top foil, which also becomes a sensor system. The foil is equipped with 18 thermocouples and 28 strain gauges. The sensors are arranged circumferentially in three parallel rows. The purpose of using so many sensors is to enable determination of the temperature and strain distributions over the entire surface of the top foil. It should be emphasized that the application of the foil-sensor required the construction of an innovative prototype of the GFB. Both the bump foils and the bearing's bushing were accordingly modified. The modification of the bump foils addressed an introduction of adequate material removal in the areas of the installed thermocouples and strain gauges in order to lead the signal wires out of the top foil. The bearing's bushing has been separated into three parts, in turn. This approach was considered to enable the folding of the top foil equipped with numerous sensors and to lead the signal wires out of the bearing's housing. To ensure the required stiffness of the bushing, it was installed making use of thrust rings, flanges and screws. The diagram showing the modifications introduced to the construction of a GFB is presented in Fig. 3.

The process of applying the sensors to the top foil of the GFB was carried out in the following steps. First, a mask for the distribution of thermocouples and strain gauges was applied to the foil in its unfolded state, i.e., for the top foil being flattened. These areas were subjected to the surface treatment process by matting and degreasing. Then, the foil was rolled and its shape fixed using dedicated holders created by the additive manufacturing method (3D printing). Strain gauges (glued with a cyanoacrylate adhesive) and thermocouples (in the form of platinum wires welded to the surface of the top foil) were installed in the test stand. The view of the prototype of the top foil with the installed sensors is shown in Fig. 4A, while Fig. 4B presents the prototype of the assembled bearing including its housing.
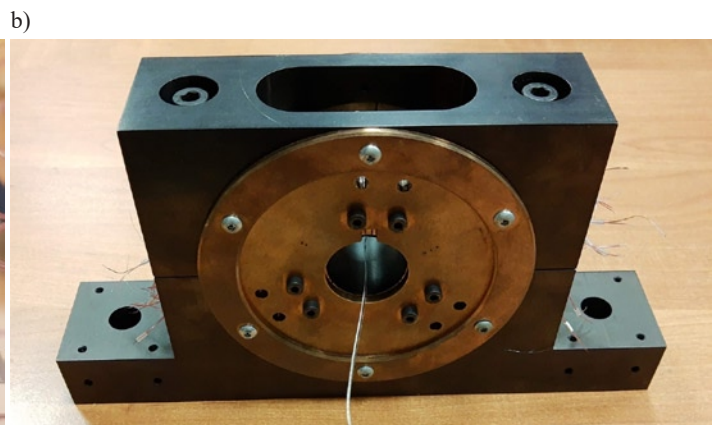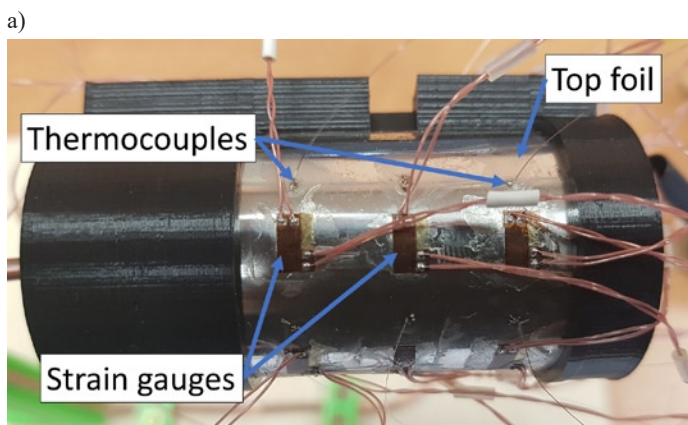
3. Numerical model of GFB

The authors have developed a numerical model of the structural parts of the GFB in order to characterize the selected mechanical and thermal properties of the top and bump foils in the bearing during its operation. From the point of view of the conducted studies, identification of the deformation of the top foil caused by simultaneously occurring and interacting sources of both mechanical and thermal loads was assumed as crucial. As part of the research, the use of the developed numerical model was considered to determine the expected contact areas between the top and bump foils and, accordingly, between the bump foil and the bearing's bushing. Moreover, the subject of the analyzes was to confirm occurrence of the increased deformations of the top and bump foil in the identified contact areas. Similarly, the areas of dominant heat propagation from the top foil to the remaining components of the GFB was also verified.

The finite element (FE) mesh of the GFB model was prepared using Altair HyperMesh software. The model takes into account the following components of the bearing: a top foil, three bump foils, a tricuspid bushing and two flanges. As an acceptable simplification of the model, the authors considered the omission of the rotating shaft and the bearing's housing in order to speed up the calculations. Due to the scope of the research closely related to the behavior of the structural part of the bearing's supporting layer, the authors assumed that the above stated approach will not significantly affect the results of the analyzes on the physical behavior of the GFB described in this paper. It should also be noted that the GFB's housing, as a part of relatively large volume and mass, is primarily a component responsible for heat accumulation. On the other hand, the presence of the rotating shaft was modeled with
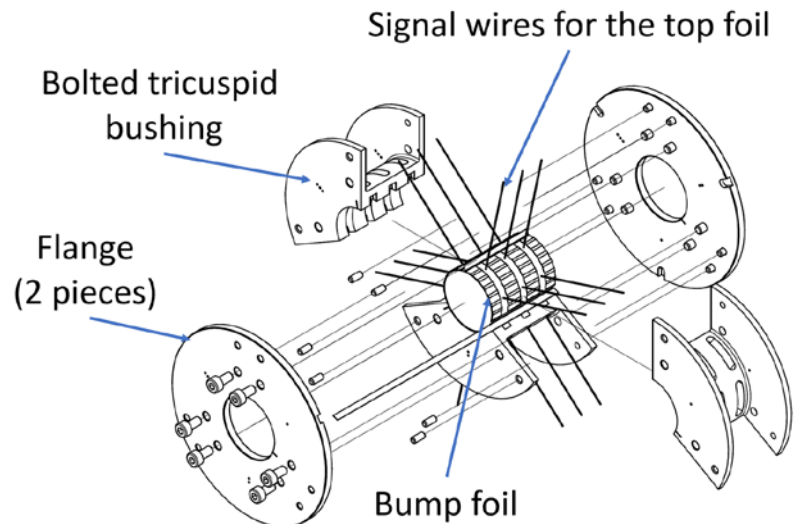

Fig. 3. Construction diagram for the GFB's components allowing to conveniently lead the signal wires out of the bearing's housing
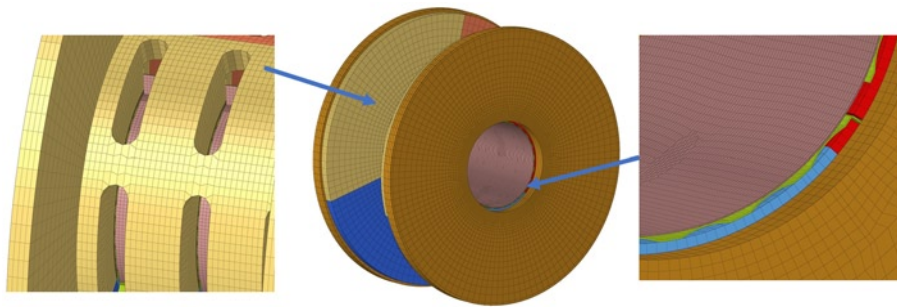

Fig. 4. View of the prototype of the top foil equipped with thermocouples and strain gauges (a) and the assembled GFB installation (b)

Fig. 5. View of the FE mesh of the GFB model

equately consider both the mechanical and thermal properties. Table 1 reports the values of material parameters considered in the FE model of a GFB.

The contact conditions configured in the model affect both the deformation of the GFB's components, but are also taken into account in the process of heat propagation in the bearing. Therefore, the FE model includes the mechanical and thermal parameters of the contact, respectively the friction coefficient of 0.03 [7] and the heat transfer coefficient for the contact area of 15000W/m²·°C [4].

the adopted pressure profile in the air film acting on the inner surface of the top foil. Therefore, the authors of the paper considered the adopted simplifications to be justified taking into account the scope of the conducted research. All FE components were modeled using three-dimensional elements. From the point of view of the desired reliability of the calculations, the top and bump foils were considered to become the key components. Both types of the foils were modeled taking into account four layers of FEs along their thickness. Due to their most complex shapes, the bump foils were modeled with the smallest FEs used in the GFB model. Their average size was set to 3mm. Slightly larger elements, i.e., with an average dimension of 5mm, were used for the top foil and in the most inner layer of the bushing elements, which are directly involved in contact with the mentioned foil. The contact model was defined appropriately between the following pairs of the GFB's components: (1) top foil and bump foils, and (2) bump foils and bearing's bushing. A general view of the constructed FE mesh and the respective close-ups are shown in Fig. 5. In total, 305,876 FEs were used in the elaborated numerical model.

The top and bump foils were modeled taking into account the properties of the INCONEL 625 material, while the properties of bronze B101 were used for the construction of the remaining components, i.e., bushings and flanges. The materials used in the model are schematically marked in the cross-section view of the FE model shown in Fig. 6.

Due to the structural mechanical and thermal phenomena included in the numerical analysis, the parameters of the materials used ad-

Table 1. Material properties used in the FE model of GFB

Material	INCONEL 625	BRONZE B101	Unit
Density	8.44	8.6	kg/dm³
Young's modulus	207.5	118.7	GPa
Poisson's ratio	0.278	0.34	-
Thermal expansion coefficient	12.8	19	10e-6 m/m·°C
Thermal conductivity coefficient	9.8	62.8	W/m·°C

The formulated calculation case considers two consecutive stages. The first stage consists of 10 calculation steps (with the time step 0.1s) and addresses a linear increase of the pressure applied on the inner surface of the top foil that represents the presence of the shaft. Moreover, fixed displacement areas are also declared in the FE model for the bushing, flanges and parts of the foils. These areas are schematically marked with pink triangles shown in Fig. 7.

The declared distribution of the pressure acting on the inner surface of the top foil is visualized in Fig. 8. This distribution was determined with the use of the computational methods of fluid mechanics developed by the research team from the Department of Turbine Dynamics and Diagnostics affiliated at the Institute of Fluid Flow Machinery, Polish Academy of Sciences in Gdańsk, Poland [2], cooperating with the authors of present publication. The highest values of the pressure occur in the central part of the top foil (along its longitudinal direction), in the region localized about half of the circumference with respect to the foils' holder area – following the direction opposite to the shaft's rotation direction.

The second stage of the conducted calculations deals with keeping the previously presented boundary conditions and additionally taking into account: (1) thermal load [2] for the top foil and (2) convection condition for the outer surfaces of the flanges. The assumed coefficient of natural convection for the air-bronze pair is 24.6W/m²·°C, referring to the data presented in [16]. In this stage of calculations, the solution is found via a single computational step representing the steady state of bearing's operation. The formulated nonlinear thermomechanical problem with contacts was solved using the MSC.Marc solver. The calculation time for the referenced stage was 4.5 hours. The calculations were performed using a workstation with the following components: Intel® Core ™ i5-8600K 3.6GHz, 32GB RAM, 500GB SSD.

4.   Results of numerical simulations

The performed numerical analyzes allowed for characterization of the selected mechanical and thermal properties of the bump and top foils for the simulated operational conditions of the GFB, i.e., for the assumed thermal and pressure excitations. One of the most interesting results obtained in the conducted simulations is identification of the regions where interactions occur in the declared contact pairs. The outcomes presented in Fig. 9 define the areas
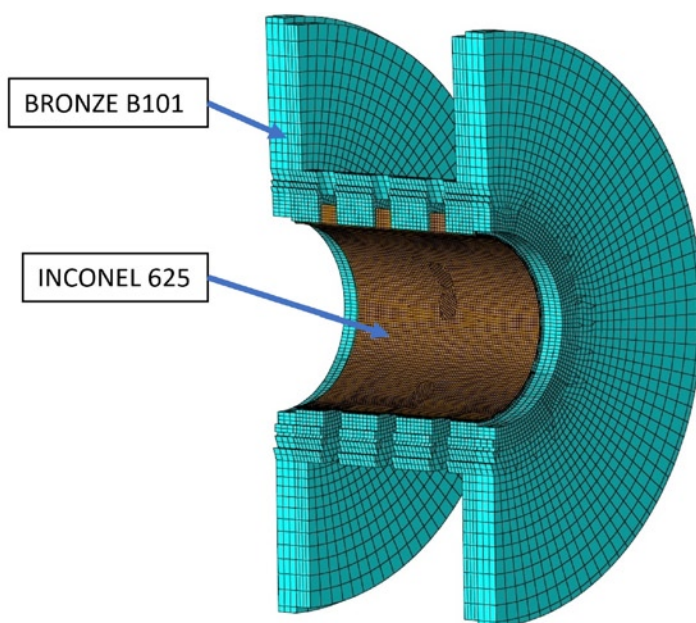

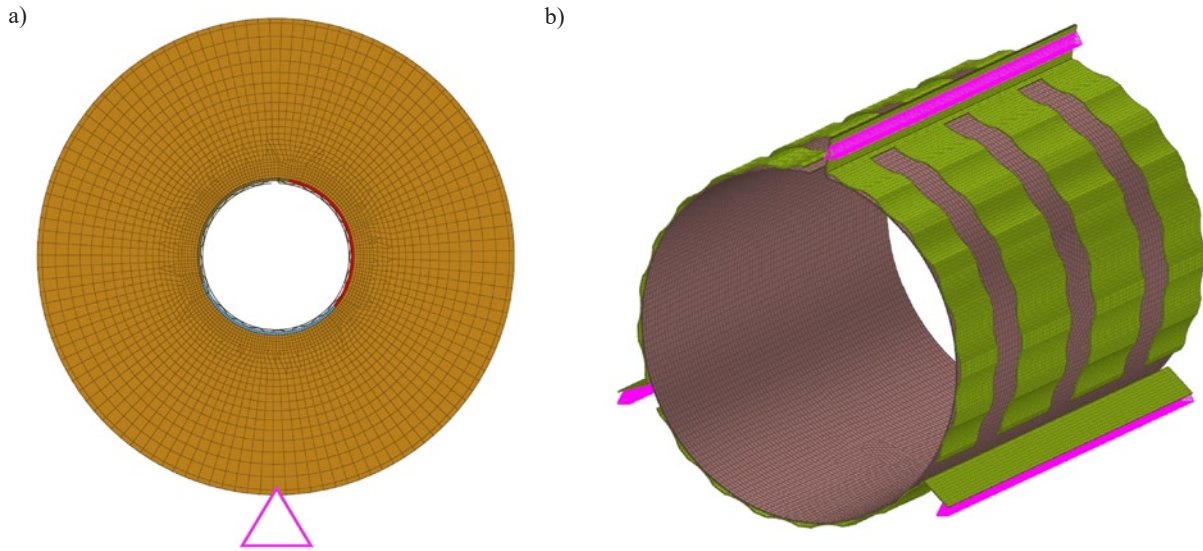*Fig. 6. A cross-section view of a FE model with marked materials*

Fig. 7. Boundary conditions – fixed displacements XYZ for all nodes of the bushing and flanges (a), and within the selected areas in the foils (b) - marked with pink triangles
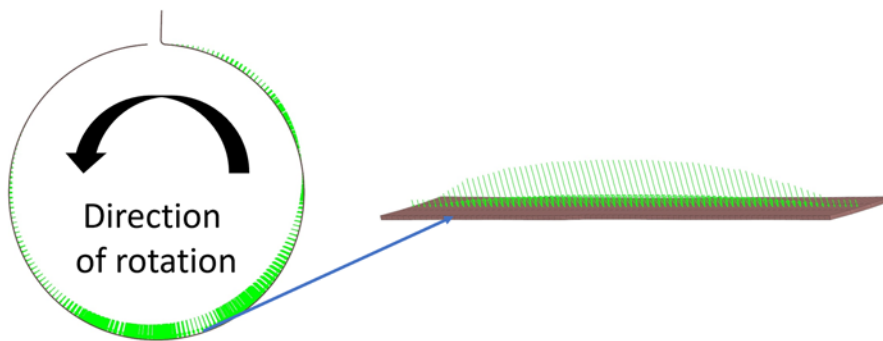

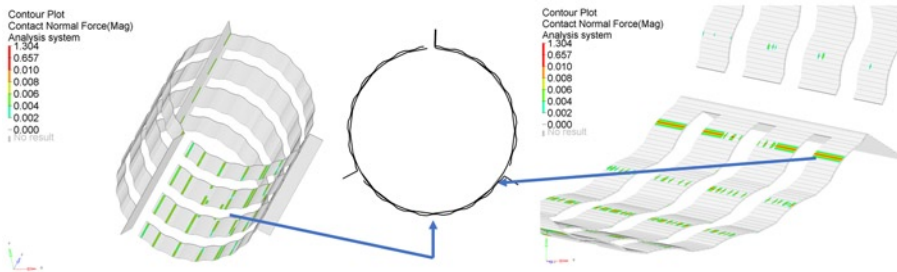*Fig. 8. Visualization of the introduced pressure distribution*

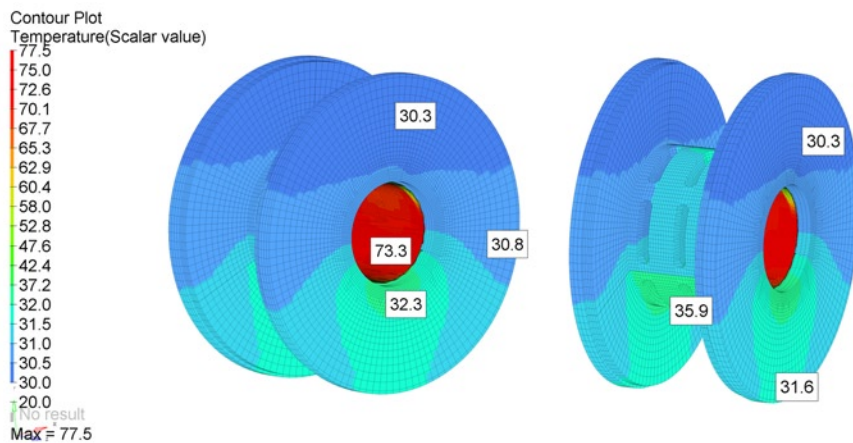*Fig. 9. Dominant areas of contacts in the GFB model identified for the assumed loads*

Fig. 10. Temperature field for the GFB's model

of registered contacts in the GFB model for the considered case study.

The greatest number of the identified contact regions relates to the bump foil lying opposite the foils' holder area. This is the region where the pressure values in the air film are the highest (for the assumed arrangement of the top foil and the direction of shaft's rotation). Contacts were identified on both the inner and outer sides of the bump foil, which corresponds to the adequate contacts with the top foil and bearing's bushing. Therefore, these locations refer to the transfer of mechanical loads identified from the shaft's journal to the bushing. On the remaining two bump foils, the number of contact areas with the top foil is much smaller. On the other hand, a tendency was observed to maintain point contacts with the bushing on the entire surfaces of the bump foils. The presented observations allow to state the conclusion that the bump foil lying opposite the foils' holder area is the component through which the heat from the top foil will propagate to the bushing at most.

The temperature distribution in the GFB model recorded in the simulations (shown in Fig. 10) confirms the above expectation. The highest temperatures were identified on the top foil of the modeled bearing. In the case of the bearing's bushing, higher temperatures were recorded in the lower part of the bearing, due to the limited heat diffusion occurring in the contact areas. In fact, according to the observations, this is the area with the greatest number of the regions of initialized contacts between the top and bump foils and, eventually, the bearing's bushing. It should be also emphasized that the differences recorded on the outer circumference of the bushing are small and amount to approx. 2°C.

Fig. 11 shows the calculated values of temperatures identified at the installation localizations of thermocouples in the prototype of the foil-sensor. To improve the clarity of the results visualization, the bushing and flanges are not visualized. It should be noted that the highest values of temperature occur for the thermocou-
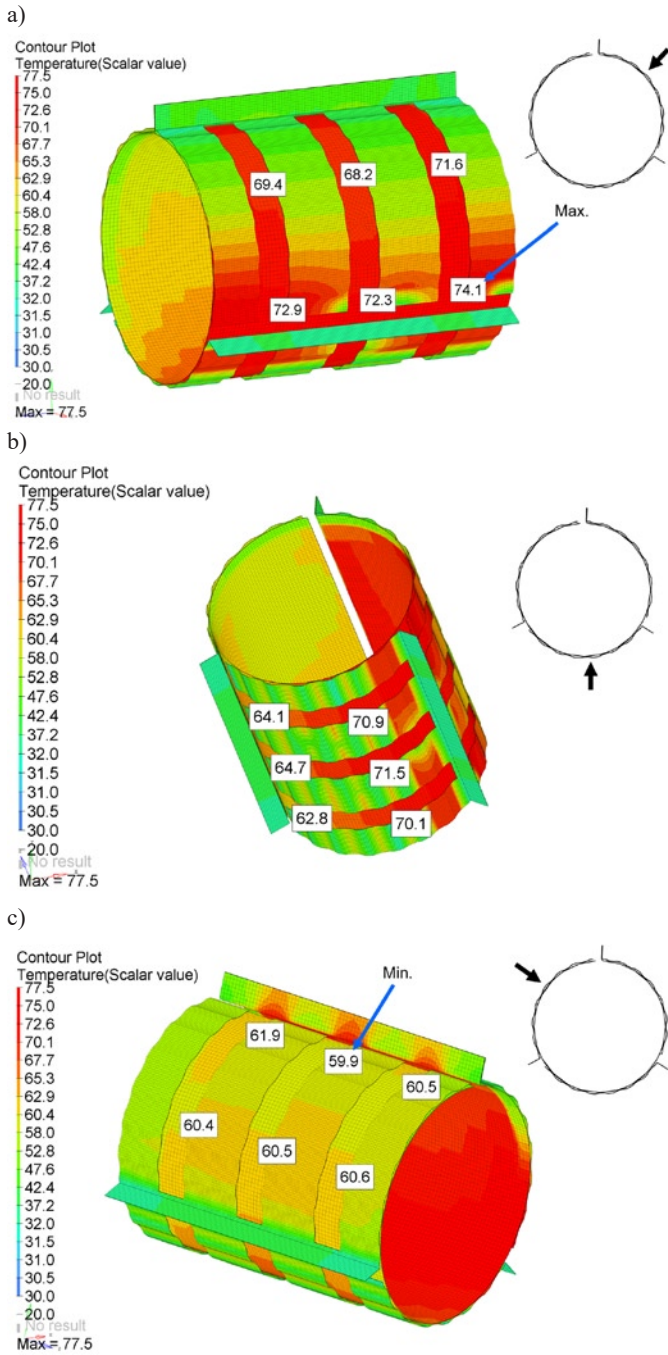
Fig. 11. Temperature field for the top and bump foils: view from the foils'
holder area (a), view of the central part of the top foil (b) and view of
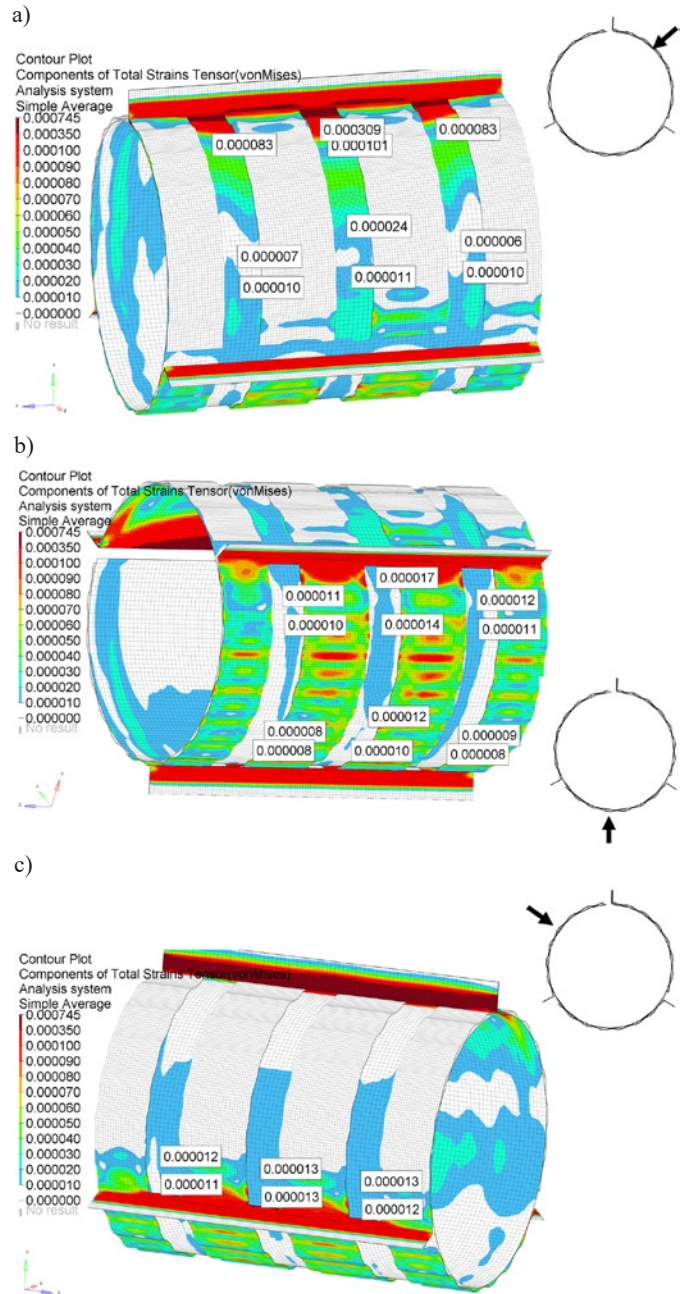the free end of the top foil (c)

Fig. 12. Huber-von Mises reduced strain field for the top and bump foils: view
from the foils' holder area (a), view of the central part of the top foil
(b) and view of the free end of the top foil (c)

ples located approximately one-third of the distance along the circumference from the foil's holder area – following the direction opposite to the shaft's rotation direction (Fig. 11a). However, the smallest values of the recorded temperatures are identified in the area of the free end of the top foil (Fig. 11C). The identified difference between the highest and the lowest temperature at the points of thermocouples installation is 24.2°C.

The strain distribution in the model components was also obtained with numerical calculations. Fig. 12 shows the area of Huber-von Mises reduced strains in the top and bump foils, identified for the analyzed case study. Again, to improve the clarity of the results visualization, the remaining model components (bushing and flanges) are not displayed. High strains can be observed in the regions where the bump foils are fixed to the GFB's bushing. Moreover, as expected by the authors, the greatest strains in the remaining areas of the bump foils were recorded in the component opposite the foils' holder area

(Fig. 12b). The mentioned component states for the region with the greatest number of activated contact points with the top foils and the bushing.

Numerical calculations carried out in the two stages allow to determine the influence of thermal interactions on the recorded strains of the top foil. The results presented in Fig. 13 show the components of the strain tensor in the strain gauges' installation areas in the model of prototype foil-sensor projected onto a plane tangent to the top foil's surface.

In the case when the pressure profile excitation is considered only, as assumed during the first stage of calculations, circumferential deformations dominate in the top foil. As far as the significant deformations along the bearing's longitudinal axis are of concern, in turn, only the area experiencing a greater number of contacts with the bump foils can be respectively indicated. Additional presence of the thermal load, as expected, tends to equalize the strain values in mutually perpendicular directions. In this case, the dominance of any of the deformation directions is not observed.
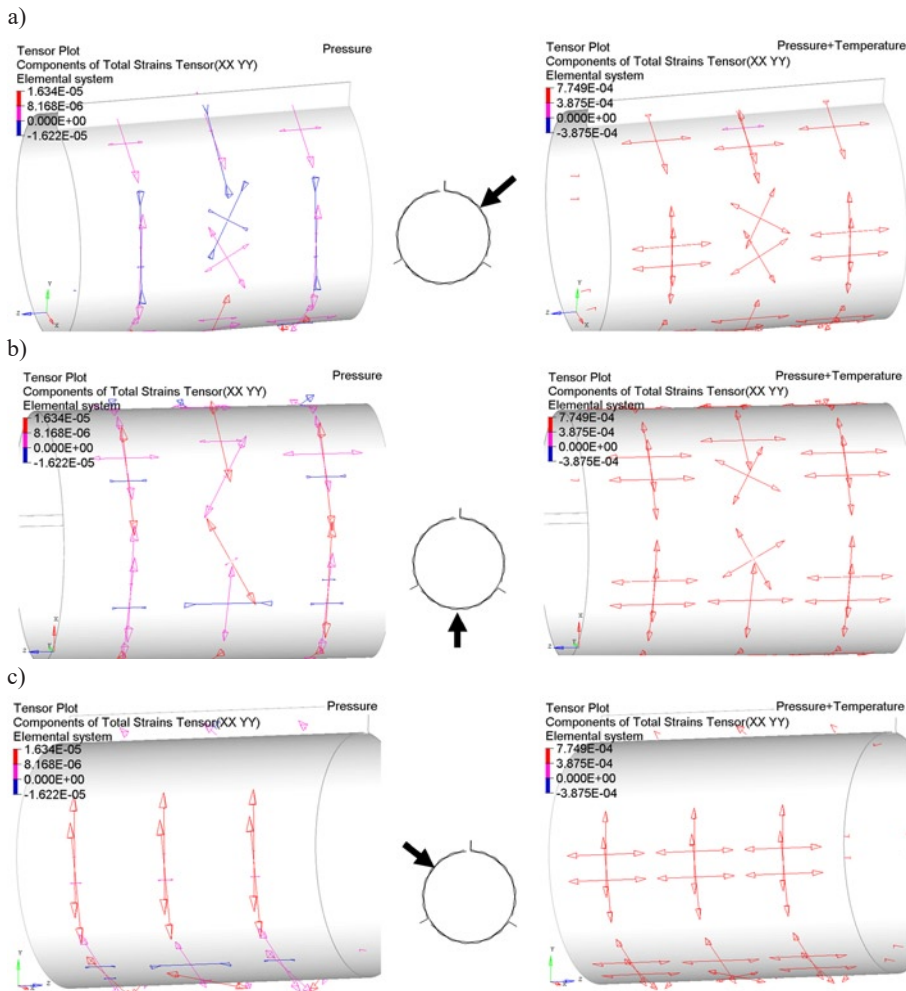
a)

b)

c)

Fig. 13. *Tangent components of the strain tensor found for the top foil at the localizations of the strain gauge installations: view from the foils' holder area (a), view of the central part of the top foil (b) and view of the free end of the top foil (c)the central part of the top foil (b) and view of the free end of the top foil (c)*

bearings, which usually operate in demanding conditions, i.e., at very high rotational speeds of the shaft. Monitoring of the operational conditions of GFBs may become an indispensable element of the system for testing the reliability of bearing installations. Considering the above statement, the authors of the present work created a prototype of a top foil equipped with 18 thermocouples and 28 strain gauges. Moreover, they expect that the specialized foil-sensor will allow for an effective identification of the temperature and strain fields during operation of the inspected bearings. The investigation on the properties of the constructed top foil prototype is, however, considered the next stage of the works carried out by the authors. In order to obtain preliminary results, i.e., the ones expected to advantageously represent the outcomes of the future planned experiments, an adequate numerical model of the GFB was created, which is presented in this paper.

The developed FE model allows, by means of computer simulations, for identification of the temperature and strain values recorded in the locations of the physical sensors mounted on a prototype top foil. The performed numerical analyzes indicated the areas of the bump foils in which there is the greatest number of contacts with the top foil and the bearing's bushing. These are also the areas through which the heat from the top foil is most intensively transferred to the bearing's bushing and other GFB's components. The temperatures determined in the conducted simulations allowed to assess the expected differences between the minimum and maximum values of the mentioned quantity readings for the thermocouples which becomes approx. 24°C. Moreover, the calculations showed that the temperature increase expected during the bearing's operation leads to equalization of the values of recorded strains of the top foil in the perpendicular directions, i.e., along its longitudinal and tangential (circumferential) directions. It should be also noted that the deformations originated from thermal expansion are an order of magnitude greater than the ones due to the introduction of the pressure profile simulating the presence of an air film. The computational model developed by the authors allows for the preliminary determination of the expected results planned to be gathered during the experimental research, which is necessary from the point of view of the correct configuration of the measurement path parameters. Finally, the experimental data will allow for validation of the currently presented numerical model.

Moreover, the values of the identified strains when both thermal and mechanical interactions are introduced, with the maximum strain of 0.000775, are an order of magnitude greater than in the case when only the pressure profile is considered - then the maximum strain amounts to 0.000016 respectively.

5. Summary and conclusions

Development of the systems allowing for a more comprehensive and reliable understanding of the operational conditions of GFBs is a current research issue. Ultimately, the developed methods and technical solutions can be used to control the behavior of the mentioned

References

1. Ambrożkiewicz B, Syta A, Meier N et al. Radial internal clearance analysis in ball bearings. Eksploatacja i Niezawodnosc - Maintenance and Reliability 2021; 23(1): 42-54, https://doi.org/10.17531/ein.2021.1.5.
2. Baginski P, Żywica G. Numerical analysis of the load capacity of a gas foil bearing taking into account fluid-structure interactions. Strojniski vestnik - Journal of Mechanical Engineering (SUBMITTED) 2021.
3. Bagiński P, Żywica G, Lubieniecki M, Roemer J. The effect of cooling the foil bearing on dynamics of the rotor-bearings system. Journal of Vibroengineering 2018; 20(2): 843-857, https://doi.org/10.21595/jve.2018.19772.
4. Celik M, Devendran K, Paulussen G et al. Experimental and numerical investigation of contact heat transfer between a rotating heat pipe and a steel strip. International Journal of Heat and Mass Transfer 2018; 122: 529-538, https://doi.org/10.1016/j.ijheatmasstransfer.2018.02.009.

5. Gu Y, Ren G, Zhou M. A fully coupled elastohydrodynamic model for static performance analysis of gas foil bearings. Tribology International 2020; 147(October 2019): 106297, https://doi.org/10.1016/j.triboint.2020.106297.

6. Ha D N, Xu Y. High Precision Manufacturing for Air Foil Bearings. Proceedings of the 6th International Conference on Nanomanufacturing, nanoMan2018, 04-06 July 2018, Brunel University London, UK 2018.

7. Kiciński J, Żywica G, Rządkowski R, Drewczyński M. Modelowanie strukturalnej warstwy nośnej łożyska foliowego. Acta Mechanica et Automatica 2008; 2(1): 45-50.

8. Kumar S, Kumar P, Kumar G. Degradation assessment of bearing based on machine learning classification matrix. Eksploatacja i Niezawodnosc - Maintenance and Reliability 2021; 23(2): 395-404, https://doi.org/10.17531/ein.2021.2.20.

9. Lai T, Guo Y, Zhao Q et al. Numerical and experimental studies on stability of cryogenic turbo-expander with protuberant foil gas bearings. Cryogenics 2018; 96: 62-74, https://doi.org/10.1016/j.cryogenics.2018.10.009.

10. Liu W, Zhao X, Zhang T, Feng K. Investigation on the rotordynamic performance of hybrid bump-metal mesh foil bearings rotor system. Mechanical Systems and Signal Processing 2021; 147: 107076, https://doi.org/10.1016/j.ymssp.2020.107076.

11. Lubieniecki M, Roemer J, Martowicz A et al. A Multi-Point Measurement Method for Thermal Characterization of Foil Bearings Using Customized Thermocouples. Journal of Electronic Materials 2016; 45(3): 1473-1477, https://doi.org/10.1007/s11664-015-4082-0

12. Martowicz A, Roemer J, Kantor S et al. Gas foil bearing technology enhanced with smart materials. Applied Sciences (Switzerland) 2021, https://doi.org/10.3390/app11062757.

13. Martowicz A, Roemer J, Lubieniecki M et al. Experimental and numerical study on the thermal control strategy for a gas foil bearing enhanced with thermoelectric modules. Mechanical Systems and Signal Processing 2020, https://doi.org/10.1016/j.ymssp.2019.106581.

14. Mazurkow A, Witkowski W, Kalina A et al. The effect of oil feeding type and oil grade on the oil film bearing capacity. Eksploatacja i Niezawodnosc - Maintenance and Reliability 2021; 23(2): 381-386, https://doi.org/10.17531/ein.2021.2.18.

15. McAuliffe C, Dziorny P J. Bearing cooling arrangement for air cycle machine. 1992.

16. Ochoa G V, Sanchez W E, Truyoll S D L H. Experimental and theoretical study on free and force convection heat transfer. Contemporary Engineering Sciences 2017; 10(23): 1143-1152, https://doi.org/10.12988/ces.2017.79124.

17. Roemer J, Lubieniecki M, Martowicz A, Uhl T. Multi-point control method for reduction of thermal gradients in foil bearings based on the application of smart materials. 7th ECCOMAS Thematic Conference on Smart Structures and Materials SMART 2015.

18. Roemer J, Zdziebko P, Martowicz A. Multifunctional bushing for gas foil bearing - Test rig architecture and functionalities. International Journal of Multiphysics 2021; 15(1): 73-86, https://doi.org/10.21152/1750-9548.15.1.73.

19. Samanta P, Murmu N C, Khonsari M M. The evolution of foil bearing technology. Tribology International 2019; 135(November 2018): 305-323, https://doi.org/10.1016/j.triboint.2019.03.021.

20. Shalash K, Schiffmann J. On the manufacturing of compliant foil bearings. Journal of Manufacturing Processes 2017; 25: 357-368, https://doi.org/10.1016/j.jmapro.2016.12.021.

21. Strzelecki S, Kuśmierz L, Ponieważ G. Thermal deformation of pads in tilting 5-pad jouranl bearing. Eksploatacja i Niezawodnosc 2008; 2: 12-16.

22. Żywica G, Bagiński P, Kiciński J. Selected operational problems of high-speed rotors supported by gas foil bearings. Technische Mechanik 2017; 37(2-5): 339-346.

23. Żywica G, Kaczmarczyk T Z. Experimental evaluation of the dynamic properties of an energy microturbine with defects in the rotating system. Eksploatacja i Niezawodnosc - Maintenance and Reliability 2019; 21(4): 670-678, https://doi.org/10.17531/ein.2019.4.17.